

Micro-porous layer with composite carbon black for PEM fuel cells

X.L. Wang^{a,b}, H.M. Zhang^{a,*}, J.L. Zhang^c, H.F. Xu^{a,b},
Z.Q. Tian^{a,b}, J. Chen^{a,b}, H.X. Zhong^{a,b}, Y.M. Liang^{a,b}, B.L. Yi^{a,b}

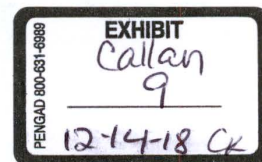
^a Fuel Cell R&D Center, Dalian Institute of Chemical Physics, CAS, Dalian 116023, China

^b Graduate School of the Chinese Academy of Sciences, CAS, Beijing 100039, China

^c Institute for Fuel Cell Innovation, National Research Council Canada, Vancouver, BC, Canada V6T 1W5

Received 11 November 2005; received in revised form 17 January 2006; accepted 17 January 2006

Available online 28 February 2006



Abstract

Effects of carbon black in micro-porous layer (MPL) on the performance of H₂/air proton exchange membrane fuel cells (PEMFCs) were studied and characterized extensively. Physical properties of gas diffusion layers (GDLs) involving surface morphology, gas permeability, hydrophilic/hydrophobic porosity and electron conductivity were examined. To construct an effective bi-functional pore structure, a novel MPL using composite carbon black consisting of Acetylene Black and Black Pearls 2000 carbon was presented for the first time. An optimal cell performance with the maximum power density of 0.91 W cm⁻² was obtained by the MPL containing 10 wt.% Black Pearls 2000 in composite carbon black.

© 2006 Elsevier Ltd. All rights reserved.

Keywords: PEMFC; Gas diffusion layer; Micro-porous layer; Composite carbon black; Hydrophilic/hydrophobic porosity

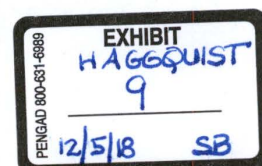
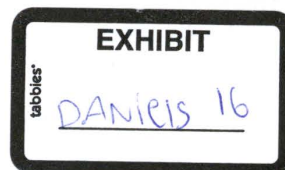
1. Introduction

Proton exchange membrane fuel cells (PEMFCs) are promising alternative power sources for stationary and mobile applications. The porous gas diffusion layer (GDL), as a component of membrane electrode assembly (MEA), plays an important role in the PEMFC by affecting the diffusion of reactants and water, and the conduction of electrons. The gas diffusion layer is typically a carbon-based porous substrate as shown in Fig. 1. The most common macro-porous gas diffusion backing (GDB) used in GDL is either carbon paper or carbon cloth, which serves as a current collector and a physical support for the catalyst layer. Micro-porous layer (MPL) consisting of carbon black powder and hydrophobic agent is applied on one side or two sides of the GDB. The function of MPL is to provide proper pore structure and hydrophobicity to allow a better gas transport and water removal from the catalyst layer, and also minimize electric contact resistance with the adjacent catalyst layer.

For the critical role in achieving high performance of PEMFC, MPL has been paid to extensive attention. Studies on the effects of the PTFE and carbon loadings in MPL were carried out [1–7]. Many other carbon blacks besides the typically used Vulcan XC-72(R) were employed to fabricate MPL [2,3,8–11]. Acetylene Black was found to be superior to others mainly because of its special characteristics involving lower surface area and pore volume. Moreover, it was found [10] that the fluoro-polymer was distributed more uniformly in MPL when using Acetylene Black and held the carbon powder particles together in a tight hydrophobic arrangement. Antolini et al. [9] suggested that employing cathode containing Vulcan XC-72 in the catalyst side and Shawinigan Acetylene Black in the gas side in MPL could optimize the cell performance at high operation pressure.

In most of the papers conducted on MPL morphology, catalyst ink was applied on GDL with painting, brushing or spraying method [2,3,8,9,11]. It is known that GDL is a porous substrate and thus the pore structure of GDL could be changed by the leaked catalyst ink. As a result, the essential features of different GDLs may be concealed to some extent. To minimize the impact of the catalyst layer, catalyst-coated-membrane (CCM) is employed in this work, in which catalyst layer is fabricated directly onto the proton exchange membrane.

* Corresponding author. Tel.: +86 411 8437 9072; fax: +86 411 84665057.
E-mail address: zhanghm@dicp.ac.cn (H.M. Zhang).



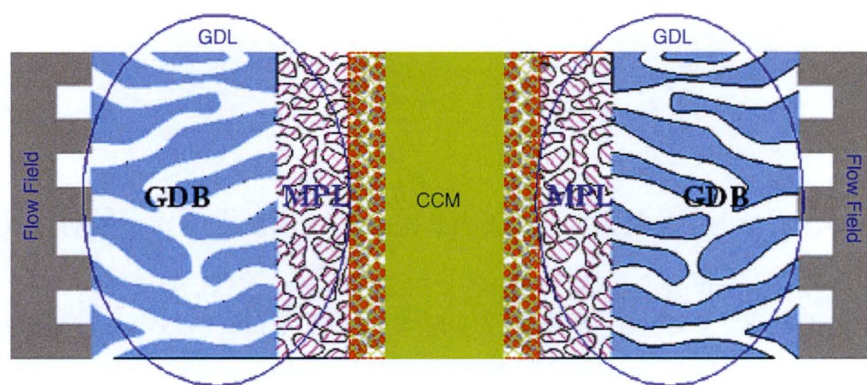


Fig. 1. Schematic of a dual-layer gas diffusion layer.

The present work aims to reveal the effects of gas and water transportation on cell performance by applying MPLs with different features. With the measurements of surface morphology, electron conductivity, gas permeability and hydrophobic/hydrophilic porosity, the key properties of different GDLs are compared. By employing cyclic voltammetry (CV) and electrochemical impedance, more information related to electrochemical reaction and mass transport with various GDLs are investigated. A novel MPL made with composite carbon powders of Acetylene Black carbon and Black Pearls 2000 carbon is described firstly. It appears to form a bi-functional pore structure permitting the good transportation for both reactant gases and liquid water.

2. Experimental

2.1. Preparation of membrane electrode assembly

Cathode gas diffusion layers were prepared using wet-proofed carbon papers (TGPH-030, Toray) as GDBs. An alcohol suspension of carbon powder and 10 wt.% PTFE emulsion stirred thoroughly by ultrasonic machine was spread onto the both sides of GDB to form a precursor of MPL, then the precursor was baked at 240 °C for 30 min, and finally it was sintered at 350 °C for 40 min. The carbon loading in each side of MPL was 0.5 mg cm⁻². PTFE content in MPL was 30 wt.% and the detail parameters of different GDLs are listed in Table 1. GDLs using Acetylene Black, Black Pearls 2000 and composite carbon black in MPL were designated as AB, BP and CC, respectively. The wet-proofed bare TGPH-030 carbon paper was denoted as CP. The anode GDLs used in the experiments were the same, with

SGL carbon papers as GDBs and Vulcan XC-72 as MPL carbon powder.

To prepare a catalyst-coated-membrane (CCM), a homogeneous mixture of Pt/C catalyst (46.1 wt.%, Tanaka), Nafion solution (5 wt.%, DuPont) and isopropanol was sprayed directly onto each side of a Nafion 1035 membrane. Nafion content in the catalyst layer was 25 wt.% and Pt loading was 0.25 mg cm⁻² for both cathode and anode. To stabilize the catalyst layer and enhance the contact between catalyst layer and membrane, the as-prepared CCM was firstly treated at 160 °C under a pressure of 1.0 MPa for 5 min, and then sandwiched between two gas diffusion layers followed by a hot-press procedure at 160 °C and 10.0 MPa for 1 min to form membrane electrode assembly (MEA). The effective area of MEA was 5 cm².

2.2. Electrochemical measurements of single cells

MEAs were evaluated in single cells at 80 °C under 0.2 MPa. The reactant gases, hydrogen and air, were externally humidified before entering the single cells by bubbling through the water at 90 and 85 °C, respectively. Constant reactant utilization of 40% for oxygen in air and 80% for hydrogen were used. The cell voltages versus current densities curves were obtained with a homemade electrical load.

The electrochemical impedance spectra (EIS) were recorded at 0.5 V in the frequency range of 100 mHz to 10 kHz with an amplitude of sinusoidal signal of 10 mV rms. A frequency response detector (EG&G Model 1025) and a potentiostat/galvanostat (EG&G Model 273A) were employed. All measurements reported in this paper were made in two-electrode

Table 1
Parameters of different gas diffusion layers

GDLs	Type of carbon powder	Total carbon loading (mg cm ⁻²)	Thickness (nm)	In-plane conductivity (mΩ cm)	Bulk porosity (%)	Permeability coefficient (×10 ¹² m ²)
AB	Acetylene Black carbon	1.0	108	6.373	70.0	1.382
BP	Black Pearls 2000 carbon	1.0	108	6.475	69.9	0.170
CC	Composite carbon black	1.0	107	6.494	69.9	1.180
CP	–	0.0	102	6.522	76.5	9.826

arrangement, with the anode serving as both counter and reference electrode and the cathode used as working electrode.

The cyclic voltammetry (CV) was performed on the electrodes using a potentiostat/galvanostat (EG&G Model 273A) at a scan rate of 50 mV s⁻¹. In the measurement of CV curves, humidified nitrogen was passed through the cathode which was served as working electrode and hydrogen were fed into the anode which was used as both counter and reference electrode.

2.3. Physical characteristics

BET surface areas, pore volumes of the different carbon powders were determined by ASAP-2010 (Micromeritics) physisorption system using N₂ as adsorbate at 77 K. The morphological characteristics of the micro-porous surface layer were examined using scanning electron microscopy (SEM, JEM-1200EX, JEOL Co.). In-plane conductivity of GDL was measured using a four-point method. The contact angles on the surface layers of desired carbon powders were tested with a sessile drop method [12].

2.4. Gas permeability

Permeability was measured by flowing nitrogen through GDL and then relating the flow rate to the applied pressure drop by means of a differential manometer. The size of each sample was 5.0 cm × 5.0 cm. Before the samples were examined, they were pressed as what had done to MEA to ensure the real pore structure at cell testing. The permeability coefficient was calculated based on Darcy's law:

$$\kappa = v\mu \frac{\Delta X}{\Delta P}$$

where κ is the permeability coefficient of a porous substrate (m²); v is the superficial velocity, calculated from nitrogen flow rate divided by the area of sample (m² s⁻¹); μ is the fluid viscosity, 1.8 × 10⁻⁵ Pa s for nitrogen at 23 °C; ΔX is the thickness of a substrate (m); ΔP is the pressure drop across a substrate (Pa).

2.5. Porosity

2.5.1. Bulk porosity

Bulk porosity of each sample was determined from an analog Archimedes measurement. In this technique, the sample was hanged and immersed in decane, which could fill both hydrophilic and hydrophobic pores [13]. The solid volume of GDL was calculated from the principle of buoyancy. Bulk porosity of GDL is defined as its total pore volume divided by the summation of its total pore volume and its solid volume.

2.5.2. Hydrophilic/hydrophobic porosity

The measurement of the hydrophilic porosity of the GDL was carried out with a homemade special apparatus. The sample was placed horizontally in the apparatus at room temperature. Water vapour carried by the air flowed through the sample. In this process, capillary condensation occurred in the hydrophilic pores inside of the GDL and the liquid water accumulated with time. By weighing the sample before and after measurement, hydrophilic porosity could be calculated. Hydrophobic porosity was decided by subtracting the hydrophilic porosity from bulk porosity.

3. Results and discussion

3.1. Physical properties of carbon powder

The physical properties of carbon powders chosen for investigation are summarized in Table 2. The surface area varies greatly from 62.0 m² g⁻¹ for Acetylene Black to 1501.8 m² g⁻¹ for Black Pearls 2000. This can be explained by the tremendous difference in pore volume and pore size distribution. The Black Pearls 2000 reveals smaller particle size and larger pore volume as compared to Acetylene Black, from which we can deduce that the MPL made of Black Pearls 2000 involves more micro-pores than that of Acetylene Black. Note that the definition of pore range is different with the general criteria. As reported by Jordan et al. [3] and Yu et al. [14], the pores in GDL are mainly in three size: macro-pores in the range of 10–100 μm, meso-pores in the range of 0.1–10 μm, and micro-pores below 0.1 μm. Composite carbon black with 80 wt.% Acetylene Black and 20 wt.% Black Pearls 2000 shows moderate characteristics between the original materials with surface area of 335.3 m² g⁻¹.

Images of water droplets on the surface of different carbon layer are shown in Fig. 2. By fitting a tangent to three-phase point where liquid surface touches the solid surface the contact angle is measured. Because there is no hydrophobic agent added, the contact angles on the surface of carbon layer imply surface characteristics of the desired carbon powders. It is obvious that the surface layer using Black Pearls 2000 with contact angle of 53° is more hydrophilic and the surface using Acetylene Black with contact angle of 153° shows stronger hydrophobicity. One reason for the phenomenon might be the more pores for Black Pearls 2000 which is in possession of high surface area and capability to adsorb water [15] relative to Acetylene Black. Another possibility is that more hydrophilic functional groups on Black Pearls 2000 resulting in the hydrophilic property. While on the interface of composite carbon black layer, contact angle of 146° is measured, which is slightly lower than that on the surface of Acetylene Black because of the adding of Black Pearls 2000.

Table 2
Physical parameters of different carbon powders

Type of carbon black	Source	Surface area (m ² g ⁻¹)	Particle size (nm)	Pore volume (cm ³ g ⁻¹)
Acetylene Black	Acetylene	62.0	42.0	0.23
Black Pearls 2000	Oil furnace	1501.8	15.0	2.67
Composite carbon	—	335.3	—	0.72

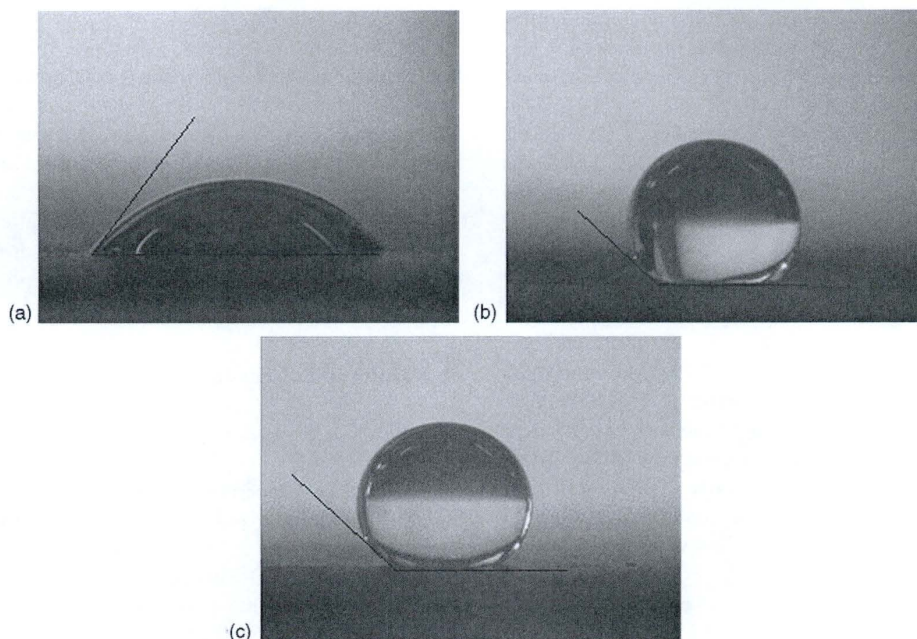


Fig. 2. Contact angles on the surface layer of: (a) Black Pearls 2000; (b) Acetylene Black; (c) composite carbon black.

3.2. Effects of different carbon powder on MPL

Single cell performance of MEAs with various GDLs was compared as shown in Fig. 3. At potential of 0.15 V, electrode with AB shows current density of 1800 mA cm^{-2} which is obviously higher than that of BP with 1000 mA cm^{-2} . The difference arises mainly from the mass transport through each GDL because all the related factors are identical including CCMs, anodes, cell assembling pressures and operating conditions. And also there is little difference in conductivity of each GDL as listed in Table 1. SEM images of MPLs with different carbon powders at 500 magnifications are displayed in Fig. 4. MPL with Acetylene

Black shows a homogeneous surface with rich pores formed by the small aggregates of carbon powders and PTFE. In contrast, MPL using Black Pearls 2000 presents a stronger compactness of carbon and a few larger cracks due to its smaller pore size. Based on the analysis of the properties of original carbon powders and the SEM images, we believe that there are many more hydrophobic macro- and meso-pores in AB, which is beneficial to the gas diffusion and reduces the mass transport limitation. On the other hand, the micro-pores provided by AB should be less and the liquid water removal by capillary-driven force would be hindered. This would be a potential factor to restrict cell performance especially at high current density region. On the contrary, BP shows more hydrophilic micro-pores serving as water flow paths, but most of them adsorb water internal leading to serious “water flooding”. The deductions will be further verified in the consequent sections.

To maintain the requirements of the well transportation of gases and liquid water, a novel GDL fabricated with composite carbon black (80 wt.% Acetylene Black and 20 wt.% Black Pearls 2000) is suggested by combination the advantages of AB and BP. The SEM photograph of CC is shown in Fig. 4(c). Clearly, the pore structure appears to be more uniform and has finer pores with proper size. As expected, electrode using CC presents the best performance with current density of 2000 mA cm^{-2} at potential of 0.15 V. It can be attributed to the more functional pores formed, which facilitate the efficient mass transportation.

The electrochemical active surface (EAS) of Pt was detected by CV measurements to investigate the influence of GDL on CCM. The calculated hydrogen desorption charges are 104, 100 and 91 mC for electrodes with AB, BP and CC, respectively. For the identical CCM applied, there is little difference in EAS of

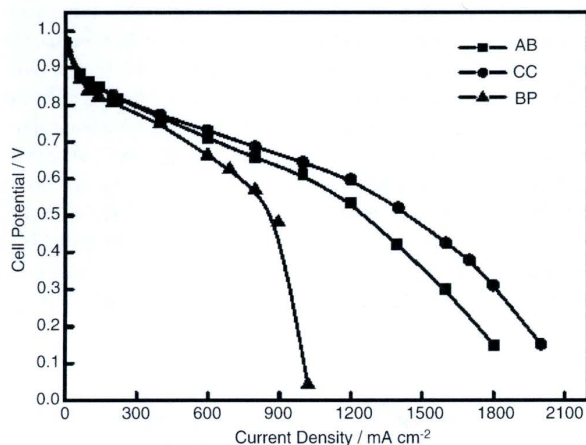
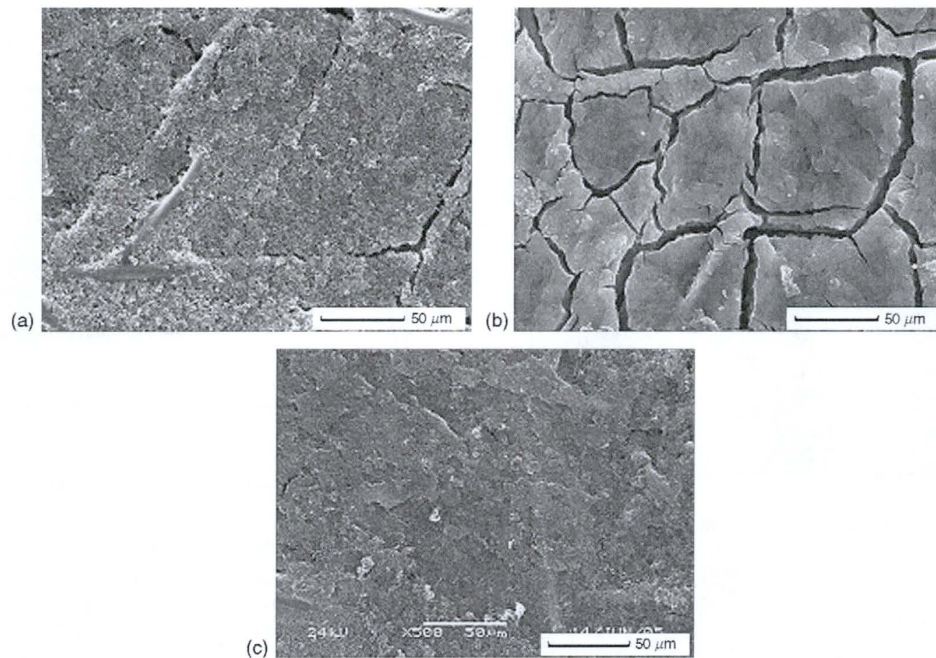


Fig. 3. Cell performance of electrodes with different MPLs for H_2/air with cell temperature 80°C , anode humidifier temperature 90°C , cathode humidifier temperature 85°C , pressure of 0.2 MPa.

Fig. 4. Scanning electron micrographs (500 \times) of: (a) AB; (b) BP; (c) CC.

Pt in various electrodes, suggesting that the degree of contact between GDL and CCM has a negligible influence to the cell performance.

Electrochemical impedance spectra at 0.5 V for each electrode are shown in Fig. 5. To date, more and more researches of EIS on fuel cell indicated that the impedance loop appeared at the higher frequency was due to the double layer charging through the charge transfer resistance and the arc at lower frequency was caused by the gas-phase transport limitation [4,6,16–18]. As can be seen from Fig. 5, the impedance spectra observed for all electrodes appears two distinguishable arcs at cell potential of 0.5 V. Electrode with BP shows obviously larger oxygen reduction reaction (ORR) charge transfer resistance arc and mass trans-

port impedance arc than that of AB and CC. On the contrary, the impedance of CC demonstrates the smallest transport-related loop. The difference between polarization curves of various GDLs can be reasonably explained by the EIS results.

3.3. Gas permeability measurement of different GDLs

Gas permeability is expected to correlate with the through holes which serve as mass transport paths when cell working. Comparison of permeability coefficients of GDLs and wet-proofed bare carbon paper is demonstrated in Fig. 6. It is evident that an addition of micro-porous layers to the macro-porous CP decreases the through-plane permeability significantly. BP

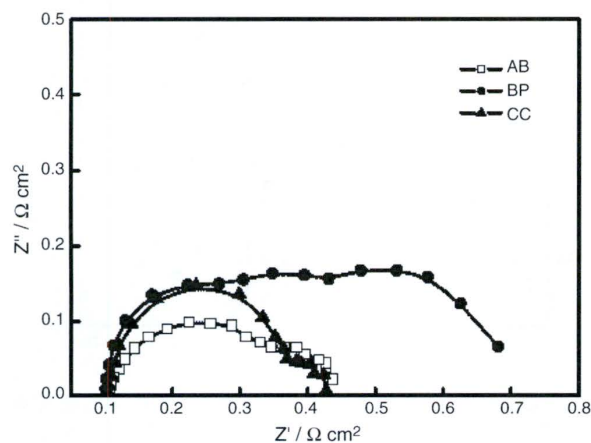


Fig. 5. Impedance spectra for electrodes with different MPLs at 0.5 V.

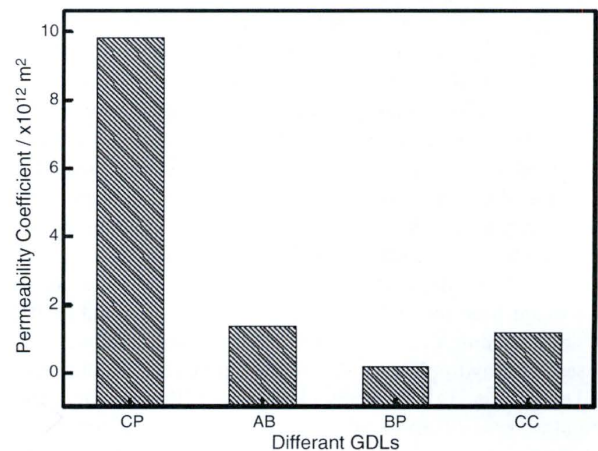


Fig. 6. Gas permeability of different GDLs.

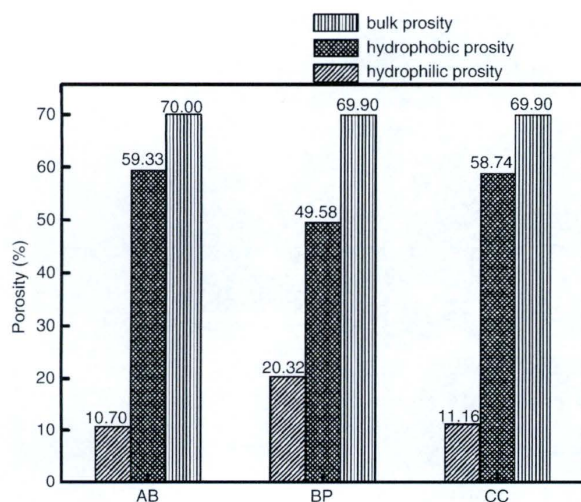


Fig. 7. Porosity of different GDLs.

shows a quiet smaller value than AB and CC. AB exhibits high-est capability of reactants passage due to the larger pore size. CC, with composite carbon powder, presents a slight lower permeability value than AB attributing to the adding of Black Pearls 2000 with small particle size. Williams et al. revealed that a GDL with higher gas permeability had higher limiting current because higher gas permeability might increase the effective diffusion coefficient as well as enhance more convection [19]. The gained conclusion was based on the special operation conditions of lower humidity and higher temperature, where the gas transport was focused on and the influence of liquid water was eliminated to a substantial extent. In our work, over saturated system is employed to study the two-phase flow occurred in most cells. So the higher limiting current but the lower permeability of CC than those of AB could be explained by the proper pore size distribution and reasonable hydrophobicity/hydrophilicity.

3.4. Porosity measurement of different GDLs

Bulk porosity and hydrophobic/hydrophilic porosity of each GDLs and wet-proofed bare carbon paper are displayed in Fig. 7. The bulk porosity of TGPB-030 bare carbon paper without PTFE is 80.0% reported by Toray Industries, Inc. While because of the occupancy of PTFE, bulk porosity of wet-proofed bare carbon paper is decreased to 76.5%, which is coincident with the calculated value of 75.4%. It indicates that the testing method is creditable. The accession of MPLs reduces the bulk porosity dramatically from ~80% to ~70%. But it seems that there is no obvious difference in various GDLs in bulk porosity.

Fig. 8 shows the curves of water incremental ratio versus experiment time for hydrophilic porosity measurement of BP. At the beginning, the curves rise up for the water vapour condenses in the hydrophilic pores and the liquid water accumulates until such pores are completely filled. About 10 h later, no incremental water is observed, so incremental ratio keeps constantly with time going on. Repeating experiment indicates that the difference is only 1.5%. The same testing method is carried out on

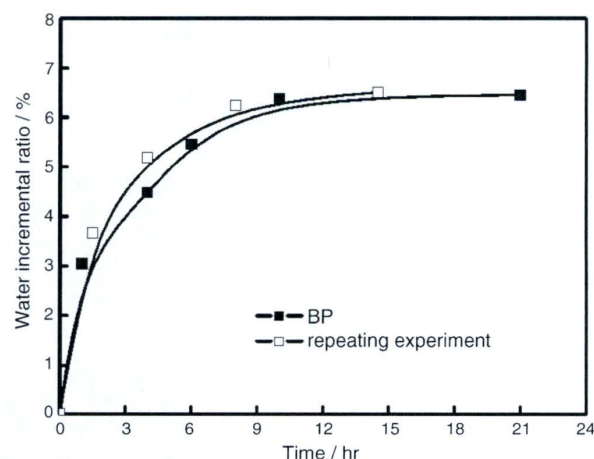


Fig. 8. Curves of water incremental ratio vs. experiment time of BP.

the other GDLs and the values for comparison are selected in the smoothing region at about 15 h. BP exhibits the highest ratio of hydrophilic pores about 20.23%, which means more pores are easy to be occupied by liquid water and relative fewer pores are left for gas transport, so the electrode with BP is intended to be “flooding”. AB shows lowest fraction of hydrophilic pores about 10.70% and more hydrophobic pores correspondingly ensures the gas transport. CC demonstrates an appropriate distribution of 11.16% hydrophilic pores and 58.74% hydrophobic pores. The flow of liquid water is improved tremendously by the little appending of hydrophilic pores compared with AB. The results suggest that the combination of two distinctive carbon powders can form a bi-functional pore structure permitting the well transportation of both reactant gases and liquid water.

3.5. Optimization of MPL with composite carbon black

Fig. 9 shows the effect of Black Pearls 2000 content in composite carbon black on the cell performance. The optimum

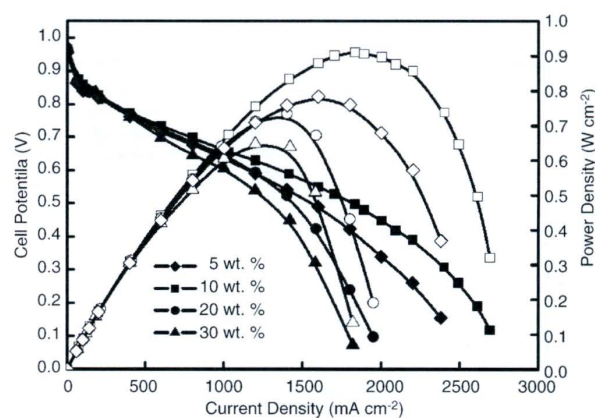


Fig. 9. Polarization curves for electrodes using MPLs for H₂/air with 5, 10, 20 and 30 wt.% Black Pearls 2000 in composite carbon black, cell temperature 80 °C, anode humidifier temperature 90 °C, cathode humidifier temperature 85 °C, pressure of 0.2 MPa.

content of 10 wt.% is obtained with the maximum power density of 0.91 W cm^{-2} . MPL with 5 wt.% Black Pearls 2000 in composite carbon black shows inferior performance to that of 10 wt.% Black Pearls 2000 content. But with the increasing content of Black Pearls 2000 up to 20 wt.% or 30 wt.%, the electrode performance is decreased because MPL with more Black Pearls 2000 is intended to be more hydrophilic and easier to be “flooding”.

4. Conclusions

Effects of carbon powders in MPL on the performance of H_2 /air PEM fuel cell are studied and characterized extensively. GDL with Black Pearls 2000 shows the lowest gas permeability and highest hydrophilic porosity of 20.32%, which leads to the serious mass polarization losses. On the contrary, GDL using Acetylene Black exhibits the highest permeability and lowest hydrophilic porosity of 10.70%, which is suitable to gas transport but not sufficient for the removal of liquid water. To form an effective bi-functional pore structure, composite carbon black consisting of Acetylene Black and Black Pearls 2000 carbon is used to fabricate MPL. An enhanced cell performance with peak power density of 0.91 W cm^{-2} is obtained by the MPL with 10 wt.% Black Pearls 2000 in composite carbon black.

Acknowledgement

This work was financially supported by the National Natural Science Foundation of China (Grant No. 50236010).

References

- [1] Z.G. Qi, A. Kaufman, *J. Power Sources* 109 (2002) 38.
- [2] L.R. Jordan, A.K. Shukla, T. Behrsing, N.R. Avery, B.C. Muddle, M. Forsyth, *J. Power Sources* 86 (2000) 250.
- [3] L.R. Jordan, A.K. Shukla, T. Behrsing, N.R. Avery, B.C. Muddle, M. Forsyth, *J. Appl. Electrochem.* 30 (2000) 641.
- [4] J.M. Song, S.Y. Cha, W.M. Lee, *J. Power Sources* 94 (2001) 78.
- [5] E. Antolini, R.R. Passos, E.A. Ticianelli, *J. Appl. Electrochem.* 32 (2002) 383.
- [6] L. Giorgi, E. Antolini, A. Pozio, E. Passalacqua, *Electrochim. Acta* 43 (1998) 3675.
- [7] J. Moreira, A.L. Ocampo, *Int. J. Hydrogen Energy* 28 (2003) 625.
- [8] E. Passalacqua, G. Squadrito, F. Lufrano, A. Patti, L. Giorgi, *J. Appl. Electrochem.* 31 (2001) 449.
- [9] E. Antolini, R.R. Passos, E.A. Ticianelli, *J. Power Sources* 109 (2002) 477.
- [10] M. Maja, C. Orecchia, M. Strano, P. Tosco, M. Vanni, *Electrochim. Acta* 46 (2000) 423.
- [11] M. Neergat, A.K. Shukla, *J. Power Sources* 104 (2002) 289.
- [12] M. Mathias, J. Roth, J. Fleming, W. Lehnert, *Handbook of Fuel Cells: Fundamentals, Technology and Applications*, 6th ed., vol. 3, Wiley, England, 2003 [Chapter 46].
- [13] M.V. Williams, E. Begg, L. Bonville, H.R. Kunz, J.M. Fenton, *J. Electrochem. Soc.* 151 (2004) A1173.
- [14] J.R. Yu, Y. Yoshikawa, T. Matsuura, M.N. Islam, M. Hori, *Electrochem. Solid-state Lett.* 8 (2005) A152.
- [15] X. Wang, I.M. Hsing, P.L. Yue, *J. Power Sources* 96 (2001) 282.
- [16] V.A. Paganin, C.L.F. Oliveira, E.A. Ticianelli, T.E. Springer, E.R. Gonzalez, *Electrochim. Acta* 43 (1998) 3761.
- [17] M. Ciureanu, R. Roderge, *J. Phys. Chem. B* 105 (2001) 3531.
- [18] Z. Xie, S. Holdcroft, *J. Electroanal. Chem.* 568 (2004) 247.
- [19] M.V. Williams, H.R. Kunz, J.M. Fenton, *J. Electrochem. Soc.* 151 (2004) A1617.